Arch. Mech. Tech. Mater.Vol. 36 (2016) 51-58

DE GRUYTER OPEN

Archives of Mechanical Technology and Materials
www.amtm.put.poznan.pl

Microstructure and selected properties of boronized layers produced on C45 and CT90 steels after modification by diode laser

Aneta Bartkowska[a]*, Dariusz Bartkowski[b], Damian Przestacki[c], Małgorzata Talarczyk[a]

[a] *Poznan University of Technology, Institute of Materials Science and Engineering, Pl. M. Sklodowskiej-Curie 5, 60-965 Poznan, Poland*
[b] *Poznan University of Technology, Institute of Materials Technology, Pl. M. Sklodowskiej-Curie 5, 60-965 Poznan, Poland*
[c] *Poznan University of Technology, Institute of Mechanical Technology, Pl. M. Sklodowskiej-Curie 5, 60-965 Poznan, Poland*

* *Corresponding author, Tel.: +48-616-653-572, e-mail address: aneta.bartkowska@put.poznan.pl*

ARTICLE INFO

Received 15 October 2016
Received in revised form 21 November 2016
Accepted 02 December 2016

KEY WORDS

Boronized layer
Laser remelting
Microstructure
Microhardness
Corrosion resistance

ABSTRACT

The paper presents the study results of macro- and microstructure, microhardness and corrosion resistance of C45 medium carbon steel and CT90 high carbon steel after diffusion boriding and laser modification by diode laser. It was found that the increase of carbon content reduced the thickness of boronized layer and caused change in their morphology. Diffusion boronized layers were composed of FeB and Fe_2B iron borides. As a result of laser surface modification of these layers, the microstructure composed of three areas: remelted zone, heat affected zone (HAZ) and the substrate was obtained. Microhardness of laser remelting boronized layer in comparison with diffusion boronized layer was lower. The presence of HAZ was advantageous, because mild microhardness gradient between the layer and the substrate was assured. The specimens with laser boronized layers were characterized by better corrosion resistance than specimens without modified layer.

1. INTRODUCTION

Diffusion boronizing is a thermo-chemical heat treatment, which is used to improve the properties of the surface layers of machine parts and tools exposed to wear, especially in the case of total lack of or restricted lubrication [1-7]. One of the disadvantages of boronized layers is brittleness, which may cause their microcracks or peeling. To prevent this, additional laser remelting process of boronized layer can be applied [1, 2, 6].Through the boronizing process surface layer consisting of hard borides can be produced, which increases the durability of e.g. mining tools as well as tools for cold and hot forming like dies or rolls [1-3]. Boronizing also increases wear resistance more than carburizing or nitriding [8, 9]. Boronized layers do not require additional heat treatment, but in the case of components, which work under high loads and are subjected to plastic deformation, the hardening and low tempering is required. Instead of the conventional heat treatment, the laser modification also can be used. It causes the obtaining of lower microhardness, but also reduces the hardness gradient between the surface and the substrate. This property probably increases the fracture toughness [1, 2]. The laser heat treatment consists of heating of the surface by absorption of the light radiation and then conduction of the heat to the sub-surface material, and finally rapid heat extraction to the cold substrate of material. The main advantages of laser treatment are e.g.: the ability to select laser power, precision of the heat delivery to the treatment place, the possibility of conducting the treatment in hard to reach places, the possibility of conducting the treatment of large surfaces also with irregular shapes [2, 4, 7, 9-19]. The group of materials that must have high surface hardness and wear resistance includes tool steels. To improve the properties of the starting material, the laser heat treatment was carried out. The authors of [17] studied the HS6-5-2 high speed steel after laser remelting and after conventional treatment. They found that laser remelting process resulted in the fragmentation of microstructure and uniform

DOI: 10.1515/amtm-2016-0010

distribution of fine-dispersion carbides. It was also observed that the microstructure of the remelted zone is non homogeneous. It was suggested that the reason of this may be a temperature gradient and differences in the mobility rate of the solidification front and movement of metal into a liquid state. Laser remelting is also applied to other kinds of diffusion layers like carburized and nitrided [9, 18]. In the paper [2] microstructure and selected properties of boronized steel after laser remelting were studied. It was found that the surface layer has a lower microhardness and the mild microhardness gradient from surface to the substrate in comparison to conventional treatment. The author moreover noted the improved wear resistance [2].
Similar conclusions were reached by the authors of studies described in [15]. They found that the laser heat treatment improves the properties of the boronized layer. The authors showed that the minimum laser beam power enabling the melting and breakdown of needle-like boride structure was 200 W. Complete removal of the directivity structure occurs at a laser power of 250 W. In the microstructure of the remelted zone, Fe_2B, Fe_3C and Feα phases were detected. It was found that as a result of remelting, both microhardness and its gradient on the cross-section were reduced [15].
The aim of this study was to determine the influence of carbon content on the macro- and microstructure, microhardness and corrosion resistance of boronized layers on steels C45 and CT90 after laser modification.

2. METHODOLOGY OF RESEARCH

The studies were carried out on the specimens made on C45 medium-carbon structural steel and on CT90 high-carbon tool steel. Chemical composition of these materials were shown in Table 1.

Table 1. Chemical composition of C45 and CT90 steels [% wt]

Steel grande	C	Si	Mn	Ni	P	S	Cr
C45	0.46	0.21	0.71	0.08	0.011	0.009	0.07
CT90	0.89	0.26	0.30	0.03	0.008	0.009	0.13

In the first step, the specimens were boronized using gas-contact method in the EKabor® powder mixture at a temperature of 900°C for 5h. In the next step the boronized layers were modified using laser beam (laser modification). In order to perform the laser heat treatment, the TRUDIODE 3006 diode laser with a nominal power of 3 kW was used. This device was integrated with the robot arm from KUKA. The parameters of the laser heat treatment were as follows: laser beam power density q = 63.69 kW/cm², scanning laser beam velocity v = 3 m/min and laser tracks overlap - 50%. The individual steps of the laser heat treatment process were shown in Figure 1. The diagram of remelting of the surface layer by the laser beam is shown in Figure 2.
Macroscopic tests were carried out using unaided eye, and their photos were taken using Canon PC 1587 photo camera. Microstructure observations were carried out on polished cross-sections of specimens after etching in 2% HNO_3 solution. For this purpose the Metaval Carl Zeiss light microscope equipped with a Moticam 2300 3.0 MP Live camera was applied.
To determine microhardness proflies, the Zwick 3212B Vickers hardness tester was used. Indentation load of 100 G and loading time of 15 seconds were applied in these studies, based on the standard PN-EN ISO 6507-1 [20].

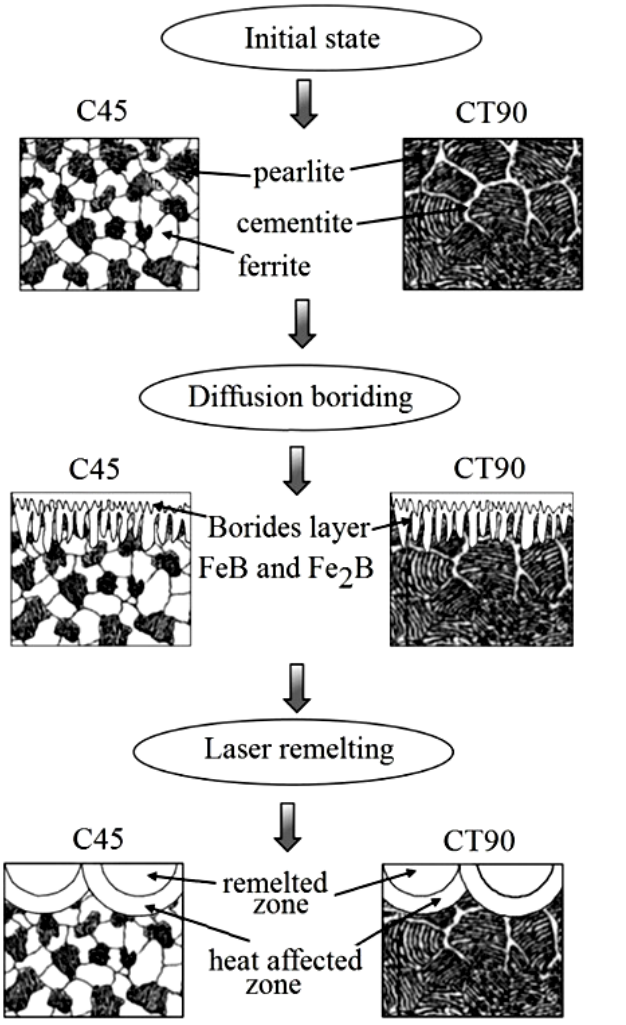

Fig. 1. Diagram of surface layer formation on C45 and CT90 steels

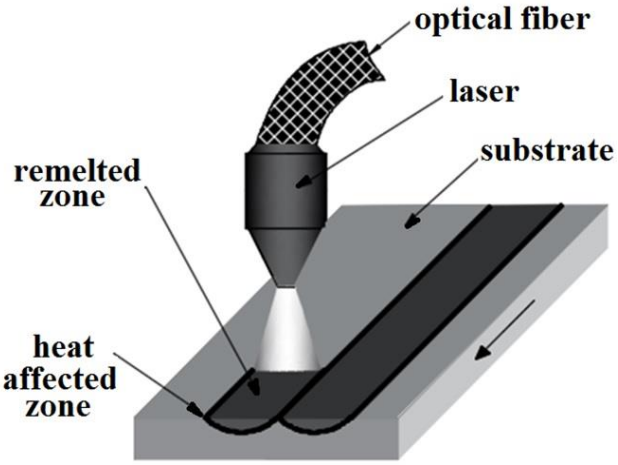

Fig. 2. Diagram of laser tracks formation process [21, modified]

Corrosion resistance studies were carried out in a 5% solution of NaCl at 22°C on the surface of 50 mm². The

studies were performed on a potentiostat-galvanostat ATLAS 0531 from Atlas Sollich company. For the determination of corrosion resistance, the potentiodynamic method was used in which the specimens were subjected to anodic polarization. Auxiliary electrode was a platinum electrode, and the reference electrode was a calomel electrode. The polarization was carried out in the range of potentials from -1.5 V to 1.5 V. The study was conducted at a rate of change in potential of 0.5 mV/s. Based on the analysis of the current, the curves of potentiodynamic corrosion and corrosion potential were determined. The corrosion resistance studies for modified surface layer of steels were carried out according to standard PN-EN ISO 17475 [22].

3. RESULTS AND DISCUSSION

Microstructure of boronized layer on C45 and CT90 steels were shown in Figure 3. The boronized layer on C45 steel (Fig. 3a) had a needle-like microstructure, wherein the needles have characteristic sharp edges and were oriented perpendicular to the surface. The substrate was composed of ferrite and pearlite. The thickness of the produced boronized layers was about 96 μm.

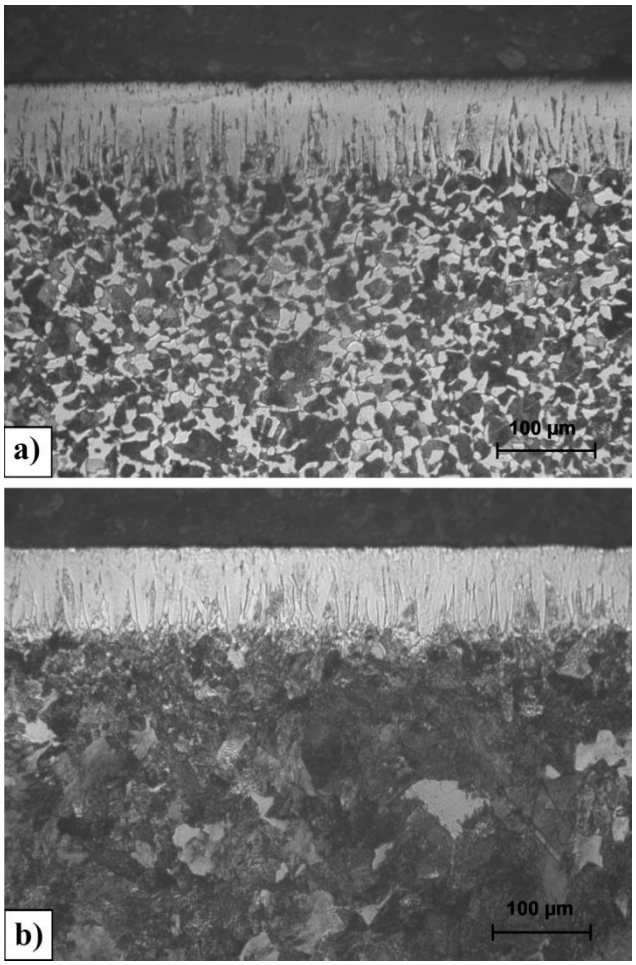

Fig. 3. Microstructure of C45 (a) and CT90 (b) steels after diffusion boriding

Figure 3b shows a boronized layer produced on CT90 high carbon steel substrate. Iron borides had a needle-like microstructure, but in contrast to the C45 steel, the needles had rounded edges. It can be concluded that the change in the carbon content of the steel substrate influences the character of boronized layer. Increasing the carbon content of the CT90 steel in comparison to the C45 steel caused the production of more continuous boride layer, and the needles were less sharp. A similar relationship was confirmed in paper [2]. The microstructure of CT90 steel occurring under the diffusion layer was composed of pearlite and cementite. The thickness of the boronized layer was approx. 80 μm, so it is less than the thickness of the layer on C45 steel. It may indicate a decreased boron diffusion rate during boronizing process as a result of the increase of the carbon content.

In Figure 4 macroscopic images of surfaces after laser modification were shown. There are clear parallel tracks resulting from a scanning of a laser beam. Irregularities on the surface were caused by the thin surface layer transition in a liquid state during the laser modification.

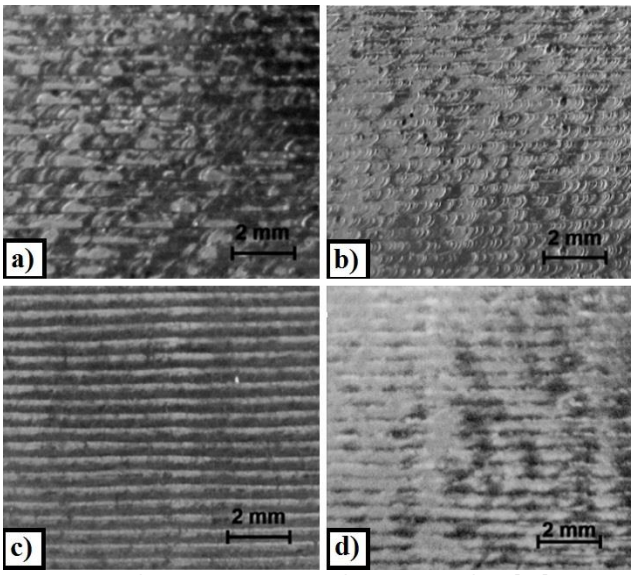

Fig. 4. Surface microstructure of specimens after the laser modification: a) laser hardened of C45 steel, b) laser hardened of CT90 steel, c) boronized laser remelting of C45 steel, d) boronized laser remelting of CT90 steel

In Figure 5 the microstructure of C45 steel after laser hardening was shown. In the cross section of the surface layer laser tracks formed after passage of the laser beam were observed (Fig. 5a). The laser tracks partially overlapped each other in 50% at the impact of the heat affected zone. In the microstructure two characteristic zones can be distinguished: remelted zone (MZ) and the heat affected zone (HAZ) (Fig. 5b). In the remelted zone, the very fine martensite was visible (Fig. 5c). This extensive fineness is associated with the rapid heat removal through a cold substrate. In the HAZ, except martensite additional ferrite occurs, which was visible as bright grains (Fig. 5d). The presence of the martensite was related with lower temperatures (less than A_3 but above the A_1), to which the material is warmed during the interaction with a laser beam. In HAZ, in overlapping track places, the microstructure had been tempered as a result of impacts of the adjacent laser beam on the already hardened area. Below of HAZ, unchanged substrate microstructure, namely ferrite and pearlite were situated (Fig. 5d).

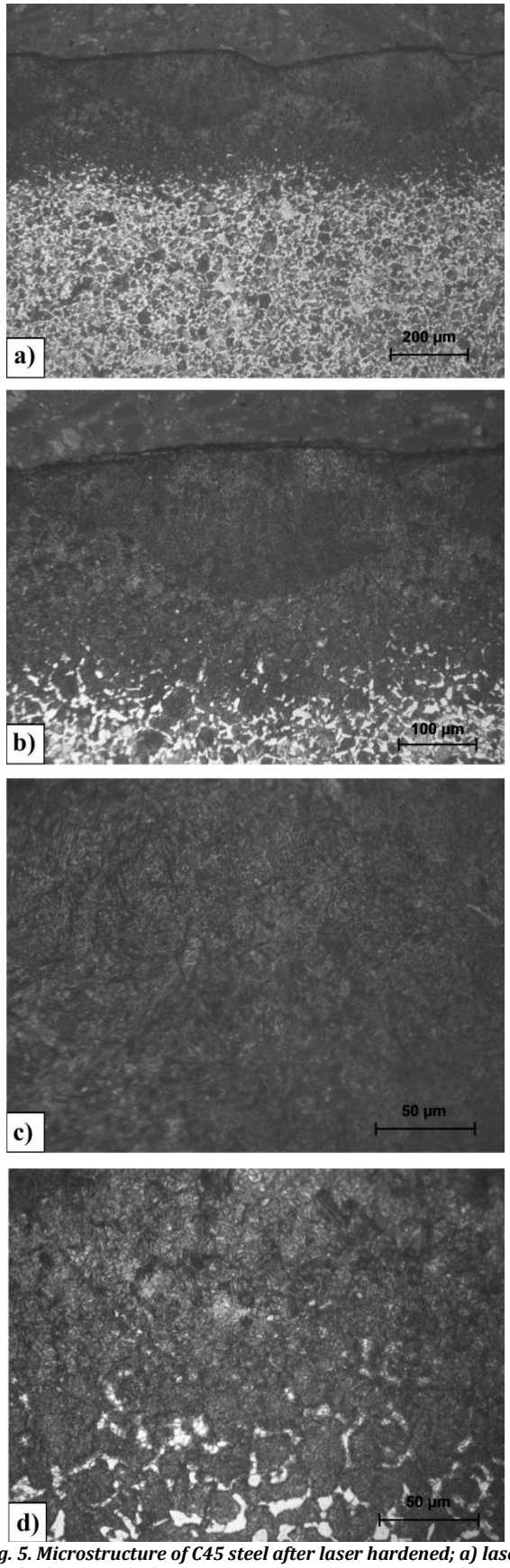

Fig. 5. Microstructure of C45 steel after laser hardened; a) laser tracks, b) magnified area 1 from figure 5a, c) magnified area 1 from figure 5b, e) magnified area 2 from Figure 5b

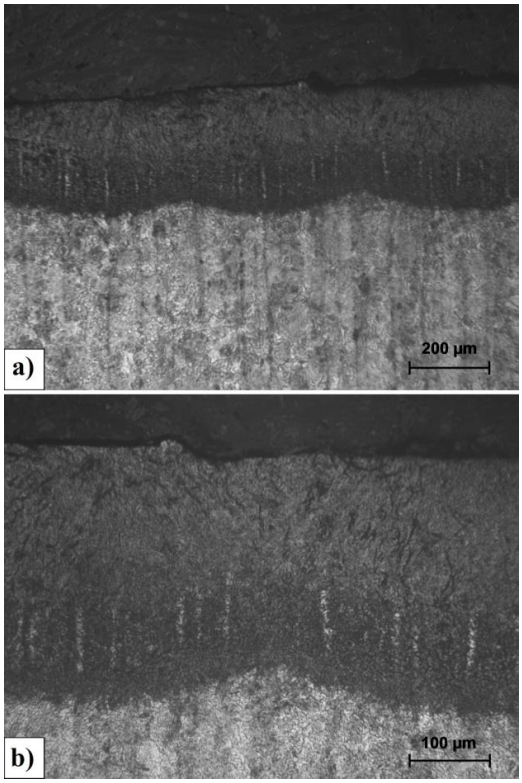

Fig.6. Microstructure of CT90 steel after laser hardening; magnification: 125x (a), 250x (b)

In Figure 6 the microstructure of CT90 steel after laser hardening was shown. Dark areas in the microstructure illustrated the laser tracks, which overlapped (Fig. 6a).

Similar to the case of C45 steel after laser hardening, the melted zone (MZ) and heat affected zone (HAZ) can be identified by the observation of the microstructure. Fine martensite was visible in the remelted zone. Due to the fact that the heat affected zone warms up to a temperature in the range from A_1 to A_{cm}, the martensite and cementite were detected there. Similar to the C45 steel, in the areas where the tracks overlapped, the microstructure was tempered. Moreover, due to the high carbon content in the steel, probably as well as in MZ and in the HAZ, the retained austenite was detected. Under HAZ the pearlite-cementite substrate was situated. In Figure 7 the microstructure of boronized layer on C45 steel after laser modification was shown. As a result of the heat impact of a laser beam on the material, the zones similar to laser hardening were created. There are remelted (MZ) and heat affected (HAZ) zones. Below these two zones the microstructure of substrate, which does not exhibit changes compared with these before treatment was detected. As a result of the laser modification the needle-like microstructere of iron boride was changed what probably influenced the increase of ductility of newly formed layer. However, on the boundary of the laser tracks areas were visible where unmelted needle-like microstructure borides were present (Fig. 7a, 7b). In remelted zone - the eutectic with dendritic microstructure (Fig. 7c, 7d), which was formed during the transition into the liquid state and re-solidification.

Dendrite axes were oriented parallel to the direction of heat removal. Microstructure of MZ in some locations had the cell microstructure. It is visible in the central part of the remelted zone in Figure 7b. At the bottom of MZ in bright areas the changes of chemical composition of microstructure are visible which are caused by the fluctuation of the melted material (Fig. 7c). Boronized layer produced on CT90 steel after laser modification was shown in Figure

8. The remelted zone and heat affected zone can be distinguished. Boronized layer was completely remelted also at the border of laser tracks, in contrast to the laser modified boronized layer on C45 steel.

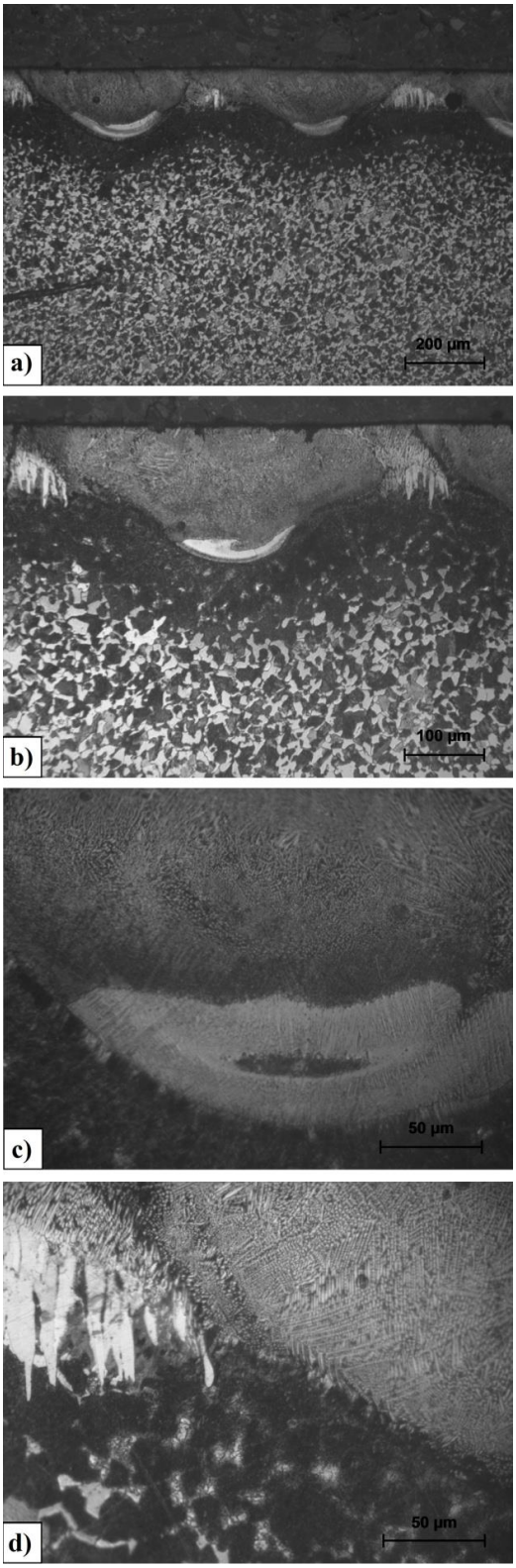

Fig. 7. Microstructure of C45 steel after laser remelting of boronized layer; a) laser tracks, b) magnified area 1 from figure 7a, c) magnified area 1 from figure 7a, d) magnified area 2 from Figure 7a

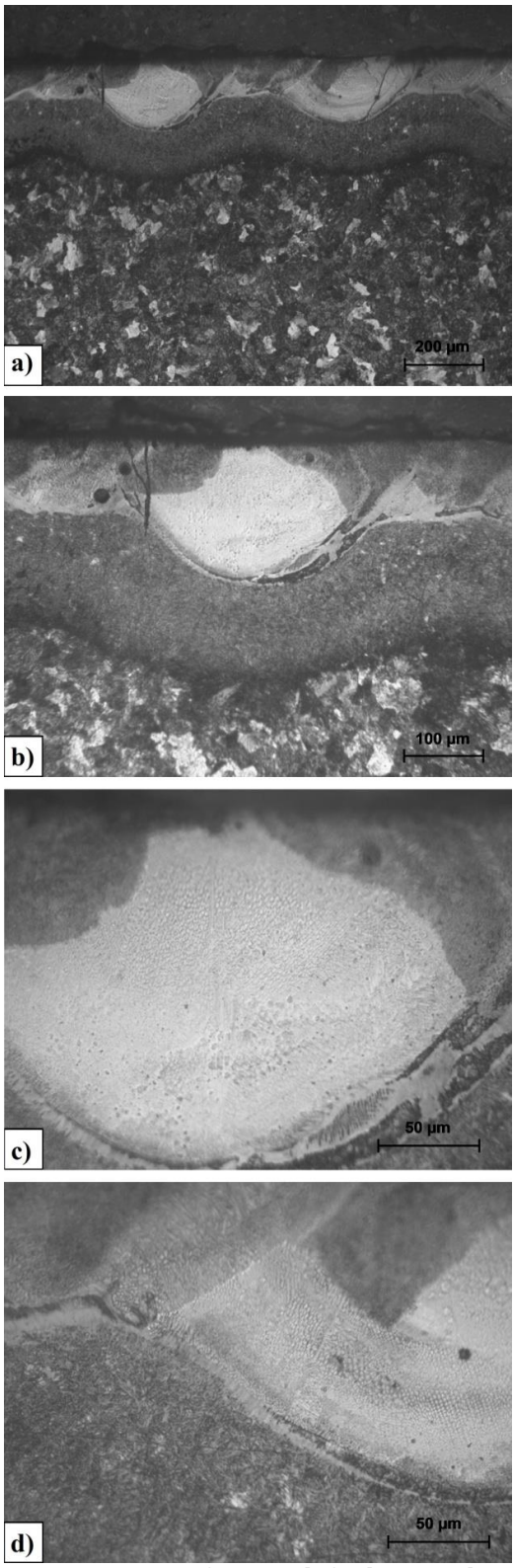

Fig. 8. Microstructure of CT90 steel after laser remelting of boronized layer; a) laser tracks, b) magnified laser tracks from figure 8a, c) magnified area 1 from figure 8a, d) magnified area 2 from Figure 8a

This may be due to the higher carbon content in the CT90 steel in comparison with C45 steel. Increasing the carbon content in steel causes the increase of heat capacity, resulting from the fact that the

carbon is characterized by higher heat capacity than iron. The heat capacity determines the time keeping warm in the impact area of the laser beam. The increase of the thermal capacity of steel causes the increase of the length of time, which probably allowed to complete the remelting of boride needles. In the area of the remelted zone, cracks and porosity were visible. Cracks most frequently occurred near the pore, directly on the boundary of laser tracks (Fig. 8a).

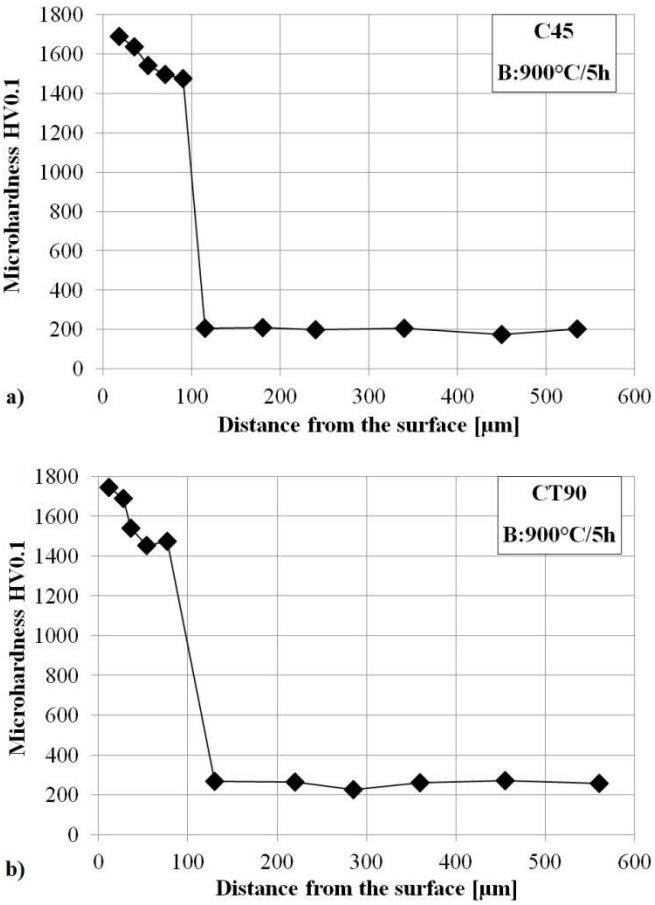

Fig. 9. Microhardness profiles of C45 (a) and CT90 (b) steels after diffusion boriding

In MZ boron-martensite eutectic mixture was present and had a cell-dendritic microstructure (Fig. 8c, 8d). The HAZ contains fine-needle martensite with cementite. Also in this case at the borders of MZ and HAZ zones, the flat solidification front was clearly visible. It was particularly visible at the highest magnification (Fig. 8c, 8d). Figure 9a shows the microhardness profile on the cross-section of C45 steel specimen after boriding. On the cross-section a high microhardness gradient between the layer and the substrate occurs. Microhardness of boronized layer was approx. 1700 HV - 1500 HV. Next the microhardness decreases rapidly to the substrate about the value of approx. 200HV. Figure 9b presents the microhardness profile of CT90 steel after diffusion boriding. Maximum microhardness in the boronized layer was 1750 HV, and it remains at the level approx. 1750 HV – 1400 HV. At the place where this layer ends, the microhardness rapidly decreases in to the substrate, and is approx. 250 HV. Boronized layer on CT90 steel had a thickness of 80 µm.

Figure 10a shows the microhardness profile of C45 steel after laser hardening. In the remelted zone the microhardness is maintained at a level of approx. 500 HV. In the heat affected zone, where a martensite microstructure containing ferrite is, the microhardness had approx. 700 HV. Higher hardness is associated with the increasing carbon content in the martensite. This area has been heated during the treatment up to a temperature ranged from A_{c3} to A_{c1} (HAZ). The lower temperature to which the material in this area is heated up, the greater content of relatively soft ferrite, but also higher saturation of martensite. This is the reason for maintaining a high degree of hardness in the range of HAZ. In the place where the HAZ ends, the microhardness decreases to a value of approx. 200-230HV in ferrite-pearlite substrate occurred.

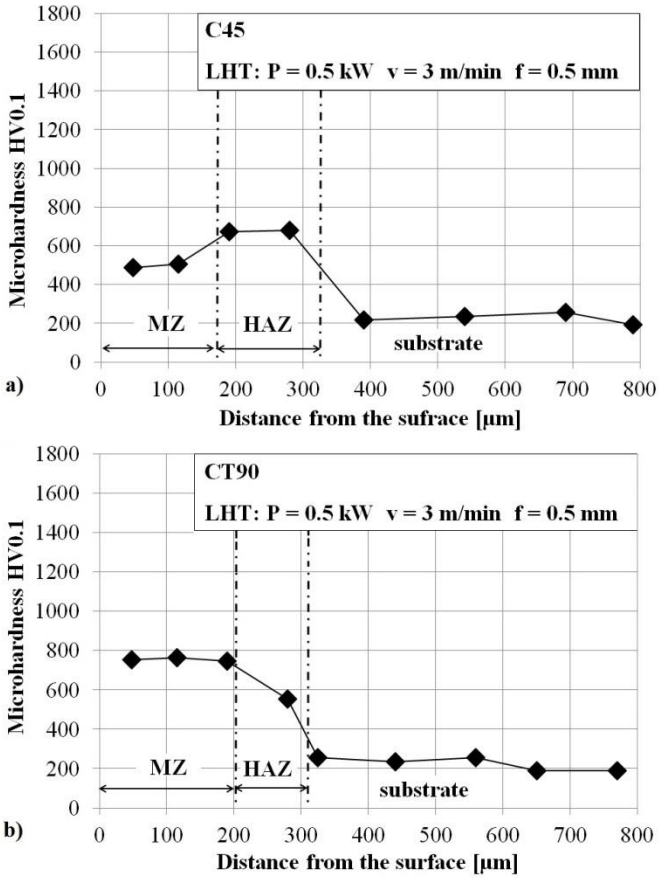

Fig. 10. Microhardness profiles of C45 (a) and CT90 (b) steels after laser hardening

Figure 10b shows a microhardness profile of CT90 hypereutectoid steel after laser modification. In the remelted zone the microhardness had approx. 780 HV. Microhardness in the heat affected zone decreases with the increasing distance from the surface from approx. 750 HV to approx. 580HV. The decrease of the microhardness in HAZ is caused by decreasing saturation of martensite with the decreasing temperature between A_{c1} and A_{cm}. At a distance of approx. 0.3 mm from the surface the substrate is located and its microhardness had approx. 200HV.

The microhardness of boronized layer produced on C45 steel after laser modification was presented in Figure 11a.

The highest microhardness occurred in the remelted zone and was approx. 1000 - 1100 HV. The microhardness on the cross-section of a sample decreases smoothly from the remelted zone to the heat affected zone (approx. 700HV), and next to the substrate (approx. 200 - 230 HV). In comparison to the boronized layers, it can be seen that the decrease of the microhardness on the cross-section is not as rapid, but the maximum microhardness is lower. Figure 11b shows the microhardness profile of CT90 steel after diffusion

boronizing and laser modification. The highest microhardness occurs within the remelted zone and it ranges close to 1100 HV. The remelted zone reaches a depth of approx. 174 μm in axis of track. Measurements of dimension of laser tracks were presented in Table 3. The microhardness of the heat affected zone was approx. 750 HV. After crossing the HAZ a decrease of microhardness occurs to approx. 200 HV in the substrate.

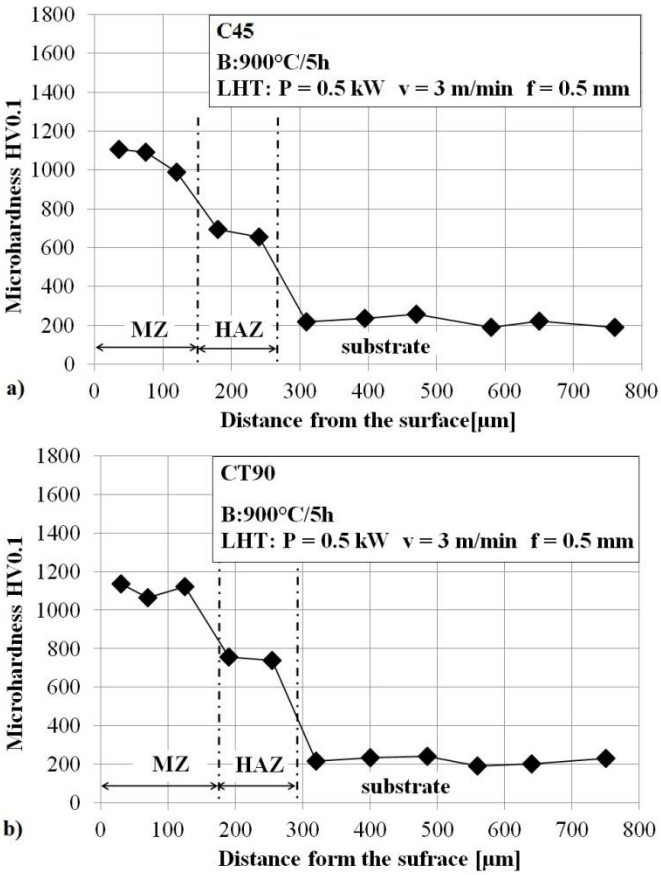

Fig. 11. Microhardness profiles of C45 (a) and CT90 (b) steels after diffusion boriding and laser modification

The results of corrosion resistance for C45 and CT90 steel specimens after laser hardened and laser remelting borided layer in 5% NaCl solution were presented in Figures 12 and 13 and in table 2.Basing on the results presented in Figure 13 and in table 2 it can be concluded that corrosion resistance after the laser modification is better for the CT90 steel in comparison to C45 steel. This is confirmed by the displacement of potentiodynamic curve for CT90 steel toward higher corrosion potential compared to the potentiodynamic curve for C45 steel. The second corrosive parameter, namely corrosion current for both of these steels is the value of the same order. Those parameters can be omitted due to the small difference between the values. In the case of specimens after diffusion boriding and laser modification, the situation was similar. The sample of CT90 steel substrate is characterized by a slightly higher corrosion resistance resulting from the higher corrosion potential relative to the C45 steel substrate.

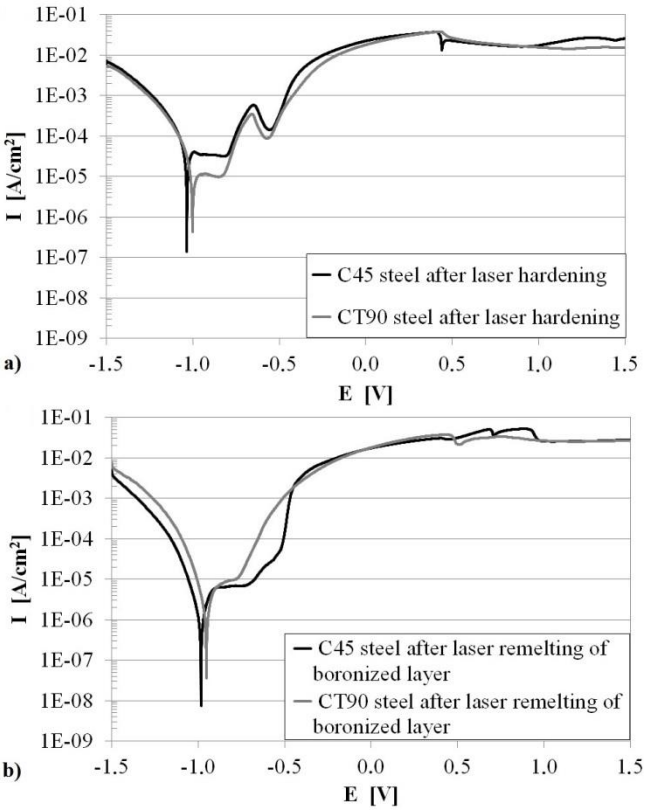

Fig. 12. Potentiodynamic curves after corrosion resistance study the C45 and CT90 steel samples after laser hardening (a) and laser modification of boronized layer (b)

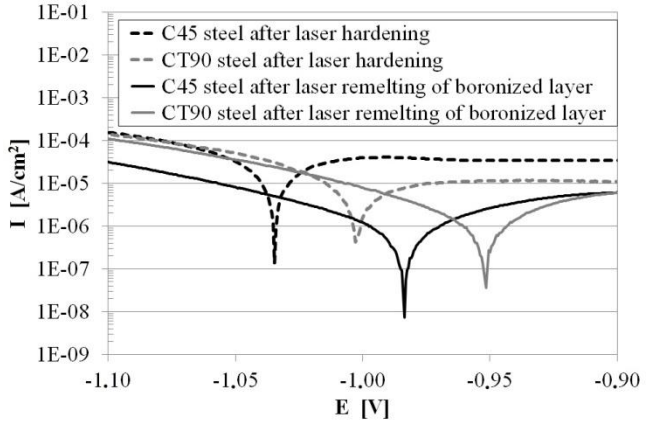

Fig. 13. Fragment of potentiodynamic curves after corrosion resistance study the C45 and CT90 steel samples after laser hardening and laser re modification of boronized layer

Table 2. Corrosion current and corrosion potential of specimens

Grade material and heat treatment	Corrosion current I_{corr} [A/cm²]	Corrosion potential E_{corr} [V]
C45 + LHT	$7.46 \cdot 10^{-6}$	-1.03
CT90 + LHT	$3.68 \cdot 10^{-6}$	-1.00
C45 + B + LHT	$2.92 \cdot 10^{-7}$	$-9.84 \cdot 10^{-1}$
CT90 + B + LHT	$4.18 \cdot 10^{-7}$	$-9.52 \cdot 10^{-1}$

4. CONCLUSIONS

The conclusions are as follows:

- The thickness of the boronized layer was higher in the substrate with lower carbon content. It suggests that the increase of the carbon content in the steel caused the decrease of the boron diffusion rate into steel.
- The carbon content influences the morphology of the boride layer. Increasing carbon content causes the rounding of the sharp ends of boride needles and the boronized layer becomes increasingly continuous.
- Laser remelting of the boronized layer reduces microhardness gradient on cross-section, because the heat affected zone is present. Using laser modification the brittleness of boronized layer can be reduced, what has a negative influence on the properties of boronized layers.
- Laser remelting of the boronized layers causes the reduction of the microhardness from approx. 1700 - 1750 HV for boronized layer to the approx. 1100 HV. However, the microhardness of laser remelting of boronized layer is higher than only laser remelting of the steel and it was approx. 500 - 780 HV.
- The carbon content in the steel affects the microhardness distribution on cross-section steel after laser remelting. In the case of C45 hypoeutectoid steel, after the laser heat treatment, microhardness in HAZ increases, whereas the microhardness of CT90 hypereutectoid steel decreases.
- The carbon content in the steel does not cause significant changes in microhardness distribution on the cross-section of a sample after boriding and subsequent laser remelting.
- Better corrosion resistance was shown in samples after boriding and laser remelting in comparison to the sample after laser hardening.
- No significant effect of carbon content on the corrosion resistance of studied samples was found (marginally better corrosion resistance was shown in samples with a substrate of higher carbon content).

REFERENCES

[1] **Przybyłowicz K.,** Teoria i praktyka borowania stali. Wyd. Politechniki Świętokrzyskiej, Kielce, 2000.

[2] **Pertek A.,** The Structure Formation and the Properties of Boronized Layers Obtained in Gaseous Boriding Process, Dissertation no. 365, Publishing House of Poznan University of Technology, Poznan, 2001.

[3] **Muhammad W.,** Boriding of high carbon high chromium cold work tool steel. IOP Conference Series: Materials Science and Engineering, 60 (2014) 1-6.

[4] **Pertek A., Kapcińska-Popowska D., Bartkowska A.,** Wpływ borowania dyfuzyjnego na mikrostrukturę i wybrane właściwości stali konstrukcyjnej. Journal of Research and Applications in Agricultural Engineering, 1 (2013) 147–150.

[5] **Uslu I., Comert H., Ipek M., Ozdemir O., Bindal C.,** Evaluation of borides formed on AISI P20 steel. Materials and Design, 28 (2007) 55 – 61.

[6] **Calik A., Simsek M., Karakas M.S., Ucar N.,** Effect of boronizing on microhardness and wear resistance of steel AISI 1050 and chilled cast iron. Metal Science and Heat Treatment, 56 (2014) 89 – 92.

[7] **Bartkowska A., Swadźba R., Popławski M., Bartkowski D.,**Microstructure, microhardness, phase analysis and chemical composition of laser remelted FeB-Fe_2B surfacelayersproducedon Vanadis-6 steel. Optics&LaserTechnology86(2016)115–125.

[8] **Balandin Yu. A.,** Boronitriding of die steels in fluidized bed. Metal Science and Heat Treatment, 46 (2004) 385-387.

[9] **Pertek A., Kulka M.,** Microstructure and properties of composite (B+C) diffusion layers on low-carbon steel. Journal of Materials Science, 38(2003) 269-273.

[10] **Kusiński J., Kąc S, Kopia A., Radziszewski A, Rozmus-Górnikowska M., Major B., Major L., Marczak J., Lisiecki A.,** Laser modification of the materials surface layer – a review paper. Bulletin of the Polish Academy of Sciences Technical Science, 60 (2012) 711–724.

[11] **Marimoto J., Ozaki T., Kubohori T. Marimoto S., Abe N., Tsukamoto M.,** Some properties of boronized layers on steels with direct diode laser. Vacuum, 83 (2009) 185–189.

[12] **Pelletier J. M., Perque D., Fouquet F.,** Laser surface melting of low and medium carbon steels: influence on mechanical and electrochemical properties. Journal of materials science, 24 (1989) 4343–4349.

[13] **Wang Z., Zhao Q., Wang Ch., Zhang Y.,** Modulation of dry tribological property of stainless steel by femtosecond laser surface texturing. Applied Physics A, 119 (2015) 1155–1163.

[14] **Elhamali S., Etmimi K, Usha A.,** The effect of laser surface melting on the microstructure and mechanical properties of low carbon steel. World Academy of Science, Engineering and Technology, 7 (2013) 373–375.

[15] **Gopalakrishnan P., Shankar P., Subba Rao R.V., Sundar M., Ramakrishnan S. S.,** Laser surface modification of Low Carbon Borided Steels. Scripta Materialia, 44 (2001) 707–712.

[16] **Grabas B., Najgeburska M.,** Wpływ temperatury i prędkości skanowaniana szerokość ścieżki zahartowanej wiązką laserową. Mechanik, 11 (2008) 951–953.

[17] **Kąc S., Radziszewska A., Kusiński J.,** Struktura i właściwości stali HS6-5-2 po przetapianiu laserowym i konwencjonalnej obróbce cieplnej. Inżynieria Materiałowa, 5 (2005) 299–302.

[18] **Yilbas B. S., Arif A. F. M., Karatas C., Akhtar S., Abdul Aleem B. J.,** Laser nitriding o tool steel: thermal stress analysis. International Journal of Advanced Manufacturing Technology, DOI 10.1007/s00170-009-2467-z, Published online: 18 December 2009.

[19] **Bartkowska A., Pertek-Owsianna A., Przestacki D.,** Hartowanie i borowanie laserowe stali konstrukcyjnej C45. Inżynieria Materiałowa 6(2013) 610-614.

[20] **PN-EN ISO 6507–1**, Metale, Pomiar twardości sposobem Vickersa. Część 1: Metoda badań. Warszawa, 2007.

[21] **Kula P.,** Inżynieria warstwy wierzchniej. Wydawnictwo Politechniki Łódzkiej, Łódź 2000.

[22] **PN-EN ISO 17475**, Korozja metali i stopów, Elektrochemiczne metody badań, Wytyczne wykonania potencjostatycznych i potencjodynamicznych pomiarów polaryzacyjnych. Warszawa, 2010.